PROCEEDINGS OF SCIENCE

Could the TeV emission of starburst galaxies originate from pulsar wind nebulae?

Xiao-Bin Chen,[a,*] **Ruo-Yu Liu**[a] **and Xiang-Yu Wang**[a]

[a]*Nanjing University, Nanjing, China*

E-mail: xbc@smail.nju.edu.cn

While the GeV γ-rays emission of starburst galaxies (SBG) is commonly thought to arise from hadronic interactions between accelerated cosmic rays and interstellar gas, the origin of the TeV γ-ray emission is more uncertain. One possibility is that a population of pulsar wind nebulae (PWNe) in these galaxies could be responsible for the TeV γ-ray emission. In this work, we first synthesize a PWNe population in the Milky Way, and assessed their contribution to the γ-ray emission of the Galaxy, using a time-dependent model to calculate the evolution of the PWN population. Such synthetic PWN population can reproduce the flux distribution of identified PWNe in the Milky Way given a distribution of the initial state of the pulsar population. We then apply it to starburst galaxies and quantitatively calculate the spectral energy distribution of all PWNe in the SBG NGC 253 and M82. We propose that TeV γ-ray emission in starburst galaxies can be dominated by PWNe for a wide range of parameter space. The energetic argument requires that $\eta_e \times \nu_{\rm SN} > 0.01 {\rm yr}^{-1}$, where η_e is the fraction the spin-down energy going to electrons and $\nu_{\rm SN}$ is the supernova rate. By requiring the synchrotron emission flux of all PWNe in the galaxy not exceeding the hard X-ray measurement of NGC 253, we constrain the initial magnetic field strength of PWNe to be $< 400\mu$G. Future observations at higher energies with LHAASO or next-generation neutrino observatory IceCube-Gen2 will help us to understand better the origin of the TeV γ-rays emission in SBGs.

38th International Cosmic Ray Conference (ICRC2023)
26 July - 3 August, 2023
Nagoya, Japan

*Speaker

PoS(ICRC2023)815

Table 1: Overview of parameter used in the modeling of PWNe.

Parameter	**Symbol**	**Value**	***varied* range**
Particle spectrum at injection			
Injection distribution index	α	$\mathcal{U}(\alpha_{\rm min},\ \alpha_{\rm min}+1)$	
Minimum index	$\alpha_{\rm min}$		1.5 ... 2.1
Injection distribution minimum energy	$E_{\rm min}$ (GeV)		1 ... 1000
Injection distribution maximum energy	$E_{\rm max}$ (TeV)	$\mathcal{U}(200,\ 800)$	
Lepton conversion efficiency	η_e		0.1 ... 1.0
PSRs population parameters			
Braking index	n	3	
Initial spin periods	P_0 (ms)	$\mathcal{N}(50,\ 35^2)(>10)$	
Pulsar's equatorial surface Magnetic field	$\log(B_p(\rm G))$	$\mathcal{N}(12.65,\ 0.55^2)$	
Nebulae			
PWNe age limit	τ(yr)	10^5	
Nebular magnetic field initial strength	B_0 (μG)	$\mathcal{U}(50,\ 200)$	
Nebular magnetic field evolution index	δ_B	0.6	

NOTE – $\mathcal{U}(a,b)$ indicates a uniform distribution from a to b.
$\mathcal{N}(\mu,\sigma^2)$ indicates a normal distribution with mean value μ and standard deviation σ.

Table 2: The energy density $U_{\rm Rad}$ and the temperature T of the three IR components due to dust and the optical one due to stars of NGC 253 and M82 from [1].

Photon field composition	**NGC 253**	**M82**
$U_{\rm Rad}^{\rm FIR}\ (\rm eV\ cm^{-3})\ \ [T\ (\rm K)]$	1958 [40]	910 [35]
$U_{\rm Rad}^{\rm MIR}\ (\rm eV\ cm^{-3})\ \ [T\ (\rm K)]$	587 [101]	637 [87]
$U_{\rm Rad}^{\rm NIR}\ (\rm eV\ cm^{-3})\ \ [T\ (\rm K)]$	587 [345]	455 [278]
$U_{\rm Rad}^{\rm OPT}\ (\rm eV\ cm^{-3})\ \ [T\ (\rm K)]$	2936 [3858]	546 [3829]

1. TeV emission from PWN population in SBGs

In the following we will investigate whether a population of PWNe can produce the TeV emission in SBGs, and explore the parameter space of some key parameters of PWNe in SBGs.

1.1 Input parameters

In this section, we explore the influences of some main parameters of our model for each individual PWNe and the entire population.

In Table 1, we summarize the parameters and relative distribution (or the allowed range) used as initial condition for the simulation of the PWNe population.

The target photon fields in SBG also include CMB, optical photons and infrared photons, while the latter two in SBG are much stronger. By fitting the thermal emission in the range from $\sim 10^{-4}$ eV to a few eV for SBG NGC 253 and M82 and assuming that the observed emission in this band is dominated by the SBN, [1] obtain the energy density and the temperature of the three

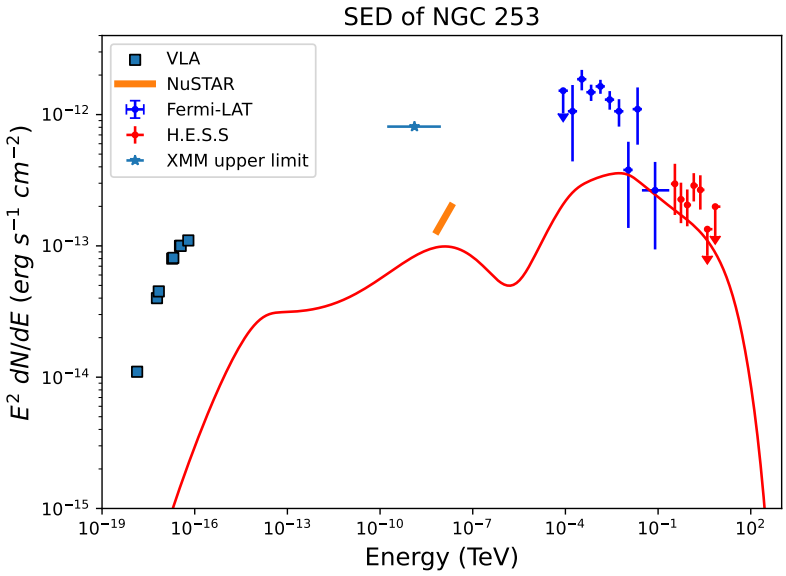

Figure 1: Predicted SED for PWNe populations in the starburst region of NGC 253 according to baseline model. Also shown is radio data from the Very Large Array [7], the X-ray point is emission from the central source X 34 as given by [8], the hard X-ray upper limit is taken from [9], the *Fermi*-LAT and H.E.S.S. data is from [10]. Horizontal error bars show the energy band over which a particular observation is made, while vertical error bars show 1σ uncertainties; the upper limits are given at 95% confidence level.

IR components due to dust and the optical one due to stars. The parameter values for each galaxies are listed in Table 2, and we use these parameter values in our calculation.

1.2 NGC 253

NGC 253 is is one of the only two starburst galaxies found to emit γ-rays from hundreds of MeV [2] to multi-TeV energies [3] . Based on the planetary nebula luminosity function, a weighted average of the most reliable distance estimates yields a distance of $d = 3.5 \pm 0.2$ Mpc by [4]. [5] derive a star-formation rate of $\sim 3.5 M_{\odot}\mathrm{yr}^{-1}$, based on the far-infrared luminosity in the starburst nucleus of NGC 253. [6] further estimate a type-II SN rate $\nu_{\rm SN}$ in the starburst nucleus of NGC 253 to be 0.02 yr^{-1}. While [3] suggest an SN rate within the starburst region of NGC 253 of $\nu_{\rm SN} \approx 0.05$ yr^{-1}, Thus, $\nu_{\rm SN}$ remains largely uncertain. Since the predicted gamma-ray flux is linearly proportional to $\nu_{\rm SN}$ and η_e, we consider $\eta_e \times \nu_{\rm SN}$ as a combined parameter.

In the following we assume all pulsars generated in the type-II SN explosions form a PWNe and evolve with age. Key parameters for estimating the flux include the typical birth period P_0 and its first order derivative $\dot{P}$ of pulsars, as the energy available for particle acceleration is $\propto \dot{P}/P^3$. $\dot{P}$ can be calculated from the equatorial surface magnetic field strength of pulsar. The PWNe population in the Galaxy is well reproduced when assuming the properties of the powering pulsars as deduced from the γ-ray-emitting pulsar population. This is due to the fact that γ-ray pulsars are representative of a younger population, and easier to generate TeV radiation. Therefore, we use the same pulsar population for starburst galaxies.

To explore the effect of key parameters $\alpha_{\rm min}$, $E_{\rm min}$ and $\eta_e \times \nu_{\rm SN}$, we test 140 ($= 7 \times 20$) different

value combinations, within the reasonable parameter space of $\alpha_{\rm min} = [1.5,\ 2.1]$ with a uniform division on a linear space, divided into 7 parts and a uniform division on the logarithmic space $E_{\rm min} = [1,\ 1000]$ GeV divided into 20 parts, respectively. For each parameter case, we simulated the generation of 5000 PWNs. The impact of $\eta_e \times \nu_{\rm SN}$ is linear and can be used for calibration.

In Figure 1, the red line shows the SED produced by a population of PWNe in NGC 253 with the so-called "baseline" model parameters, i.e. $\alpha \in \mathcal{U}(1.8,\ 2.8)$ and $E_{\rm min} = 162$ GeV. Based on the analysis in Section 1.1, we choose $\eta_e \times \nu_{\rm SN} = 0.05\ {\rm yr}^{-1}$ as an intermediate parameter to analyze. In this baseline model, the IC emission can explain the TeV emission of NGC 253 while the synchrotron emission does not exceed the X-ray limit. In the figure, the *NuSTAR* upper limit is obtained by deducting the two known hard x-ray components from the observed flux: thermal gas and X-ray binaries point sources [9] . This represents the unresolved, diffuse non-thermal emission.

In the following, we investigate the dependence of the gamma-ray flux on different choice of parameters, $\alpha_{\rm min}$ and $E_{\rm min}$. For the different parameters adopted, we use the same initial condition distribution of pulsars, and calculate the SED of NGC253, shown in the two panels of Figure 2. We choose the same $\eta_e \times \nu_{\rm SN} = 0.05\ {\rm yr}^{-1}$ for a comparison. For the injection distribution index range, we also selected other possible distributions, i.e. fixing the maximum index and variable the minimum index.

The top panel of Fig. 2 illustrates the impact of changing $E_{\rm min}$, from 1 GeV to 1000 GeV. The figure shows that the gamma flux is sensitive to the minimum energy truncation of accelerated electrons: the larger minimum energy truncation, the higher flux. The bottom panel of Fig. 2 illustrates the dependence of the results on the slope of the injection spectrum, from $\mathcal{U}(1.5,\ 2.5)$ to $\mathcal{U}(2.1,\ 3.1)$. Steeper spectra, as expected, leads to a smaller gamma-ray flux at the highest energies. As the injection spectrum softens, the flux starts declining rather steeply at energies between 0.1 TeV and a few TeV.

The allowable parameter space to account for the TeV flux of NGC 253 is shown in Figure 3, which is obtained by comparing the model and the observed flux at 1 TeV within 1σ statistical uncertainties [3]. Softer spectra at injection is allowable, if the injection efficiency η_e or the injection distribution minimum energy $E_{\rm min}$ is increased. The range of allowable parameters is very large and covers the typical values that are usually used, suggesting that PWNe are favorable to explain the very-high-energy emission from starburst galaxies. When $\eta_e \times \nu_{\rm SN} < 0.01 {\rm yr}^{-1}$, there will be almost no parameter space that can match the observed TeV flux. As long as the conversion efficiency is not too low, the very-high-energy radiation from PWNe alone can contribute dominantly to the radiation in the TeV band of the starburst galaxy.

1.3 Constraint on initial magnetic field strength of PWNe

Although the initial magnetic field strength of PWNe dose not affect TeV emission of SBG (see Section 1.1), it can affect the intensity of synchrotron radiation, so the X-ray observations can be used to constrain the initial magnetic field of PWNe.

[9] utilize the *NuSTAR* and *Chandra* data to investigate the populations contributing to the galaxy-wide 0.5-30 keV emission from NGC 253. Considering the contribution of point sources, also diffuse gas thermal emission, they determine the 90% upper limit on the flux in the 7-20 keV band. The component flux can be originated from synchrotron radiation. This determines that the

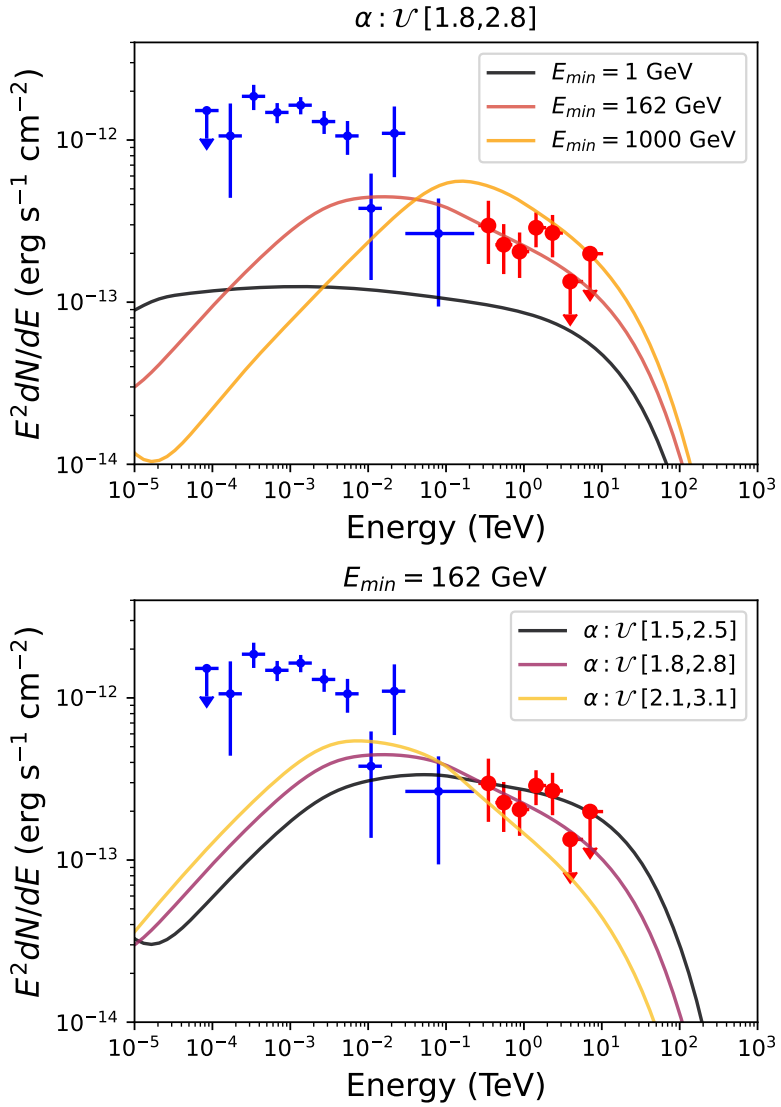

Figure 2: Predicted SED for PWNe populations in the starburst region of NGC 253. *Fermi*-LAT points are dots (blue), and H.E.S.S. points are circle (red). Single case flux calculated by changing the value of the two most relevant parameters, one for each panel.

initial magnetic field of PWNe cannot be too high, otherwise the hard X-ray emission will exceed the upper limit.

The injection spectrum of electrons determines the slope and extension of the observed spectrum. In PWNe, hard X-rays are mainly produced by synchrotron radiation, and the critical frequency of synchrotron can be defined as $\nu_c = 3eB\gamma^2/4\pi mc$. Thus synchrotron radiation of TeV electrons produces X-rays.

Due to the energy spectrum is sensitive to the electron injection spectrum, here we take $\alpha \in \mathcal{U}(1.6,\ 2.6)$ as an example to demonstrate in Fig. 4, which shows the SED under different initial magnetic fields of PWNe. In each panel, the color lines from dark to light indicate the $E_{\rm min}$

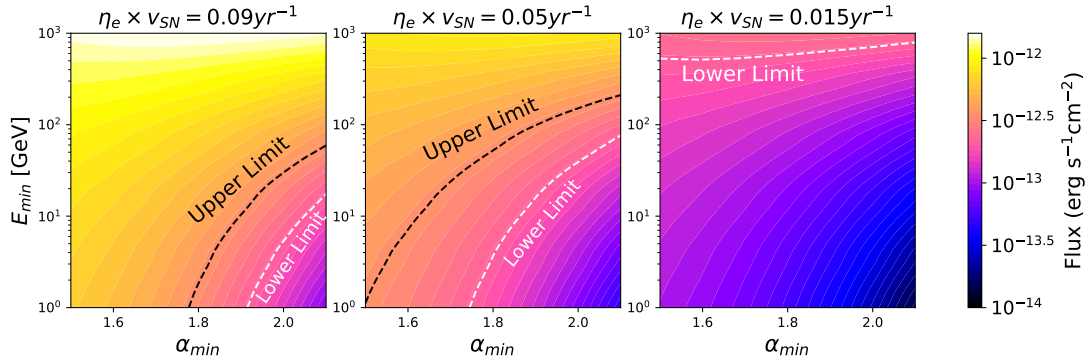

Figure 3: For NGC 253, allowable parameter space for $\alpha_{\rm min}$, $E_{\rm min}$ and $\eta_e \times \nu_{\rm SN}$. Deriving parameter ranges by limiting flux at 1 TeV with 1σ statistical uncertainty by H.E.S.S. The blue and white dashed lines represent the upper and lower limits of the 1σ respectively, and the middle area is the allowable parameter space.

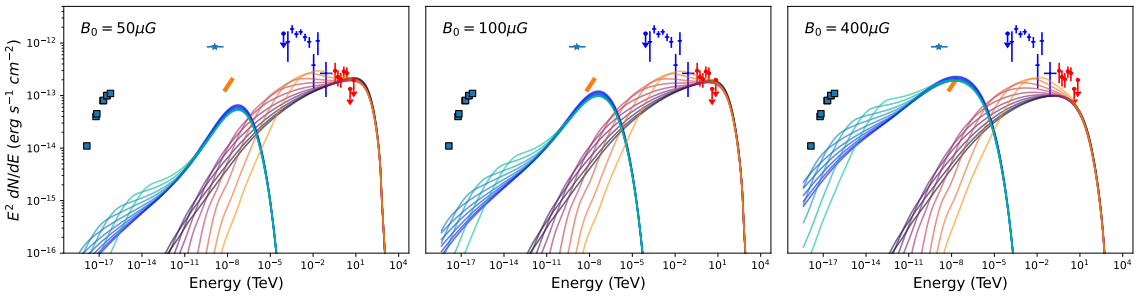

Figure 4: As Figure 1, *Fermi*-LAT points are dots (blue), H.E.S.S. points are circle (red), *NuSTAR* upper limit is line (orange), *Chandra* total radiation is star (cyan), Very Large Array points are square. The blue-purple lines with lower energy represent synchrotron radiation, and the red-black lines with higher energy represent IC radiation. In each panel, taking $\alpha \in \mathcal{U}(1.6,\ 2.6)$ as an example, the color lines from dark to light indicate the $E_{\rm min}$ cases from from 1MeV to 100GeV on the logarithmic interval, respectively.

cases from from 1MeV to 100GeV on the logarithmic interval, respectively. This also proves that the minimum energy truncation $E_{\rm min}$ does not affect the hard X-ray.

The result is dominated by two factors: firstly, due to the increase of the magnetic field, synchronous loss enhance, resulting in a corresponding decrease flux emitted by TeV IC emission. Therefore, if the TeV IC scattering achieve the observed flux, it is necessary to improve the conversion efficiency and further affect the total flux emission. The second factor is the energy spectrum of electrons. Due to normalization, as the injected energy spectrum becomes softer, the distribution of high-energy electrons is relatively reduced, resulting in a corresponding decrease in the energy of the hard X-ray band. Based on the allowable parameter space (Fig. 3) given by the limitation of the TeV band, when the magnetic field exceeds 400 μG quantitatively, to achieve the radiation observed in the TeV band and to ensure that the flux in the hard X-ray band does not exceed the upper limit given by the observation, both of these points cannot be met simultaneously.

In summary, The same electrons, which produce TeV γ-ray by IC scattering, produce X-rays by synchrotron radiation in magnetic field. Therefore, we believe that this is the upper limit of the initial magnetic field of PWNe in starburst galaxy, i.e. PWN's $B_0 < 400\mu$G.

2. Conclusion

Starburst galaxies such as M82 and NGC 253 show a much harder GeV and TeV γ-rays spectrum than that of the Milky Way, and the PWNe associated with core-collapse supernovae in starburst regions can readily explain the observed high TeV flux.

We presented a modeling of the populations of PWNe in the Milky Way, and assessed their contribution to the VHE emission of the Galaxy. Focusing on pulsar-powered PWNe, expected to be the dominant emitters in the VHE range, the mock PWNe population is to account satisfactorily for the properties of currently known PWNe in Milky Way. We then apply it to starburst galaxies and quantitatively calculate the spectral energy distribution of all PWNe in the SBG for NGC 253 and M82. Our primary results are as follows:

1. The PWNe associated with core-collapse supernovae in starburst regions can readily explain the observed high TeV luminosity of SBG NGC253 and M82. The TeV γ-ray from starburst galaxies may be dominated by a population of PWNe.

2. The current observations still impose very broad constraints on the allowable parameters of PWNe, over a wide allowable parameters range, which means the very high potential of PWNe population to explain TeV γ-ray from SBGs.

3. The energetic argument requires that $\eta_e \times \nu_{\rm SN} > 0.01$ yr^{-1}, where η_e is the fraction the spin-down energy going to electrons and $\nu_{\rm SN}$ is the supernova rate. Since the $\nu_{\rm SN}$ of SBGs is usually much higher than in other galaxies, this condition is easily met.

4. By requiring the synchrotron of the PWNe not exceeding the hard X-ray observations, we constrain the initial magnetic field strength of PWNe to be 400 μG.

In the future, for the PWN model, LHAASO might be able to measure the truncation of the high-energy IC component (extend to PeVastro), which of course requires sufficient observation time [11]. Because of the K-N effect, IC radiation would not be expected to reach higher energy bands, while the proton reaction has the potential to extend to higher energy bands, which might be a means of distinguishing between the two. And the next-generation neutrino observatory, IceCube-Gen2 can identify a cumulative signal from populations where the closest sources have up to 20 times fainter neutrino fluxes than point sources detectable by IceCube [12], thus in combination with neutrino observations, the origin of leptons/baryons emission from SBG is expected to be distinguished.

References

[1] E. Peretti, P. Blasi, F. Aharonian and G. Morlino, *Cosmic ray transport and radiative processes in nuclei of starburst galaxies*, **487** (2019) 168 [1812.01996].

[2] A.A. Abdo, M. Ackermann, M. Ajello, W.B. Atwood, M. Axelsson, L. Baldini et al., *Detection of Gamma-Ray Emission from the Starburst Galaxies M82 and NGC 253 with the Large Area Telescope on Fermi*, **709** (2010) L152 [0911.5327].

[3] H.E.S.S. Collaboration, H. Abdalla, F. Aharonian, F. Ait Benkhali, E.O. Angüner, M. Arakawa et al., *The starburst galaxy NGC 253 revisited by H.E.S.S. and Fermi-LAT*, **617** (2018) A73 [1806.03866].

[4] R. Rekola, M.G. Richer, M.L. McCall, M.J. Valtonen, J.K. Kotilainen and C. Flynn, *Distance to NGC 253 based on the planetary nebula luminosity function*, **361** (2005) 330.

[5] V.P. Melo, A.M. Pérez García, J.A. Acosta-Pulido, C. Muñoz-Tuñón and J.M. Rodríguez Espinosa, *The Spatial Distribution of the Far-Infrared Emission in NGC 253*, **574** (2002) 709 [astro-ph/0205167].

[6] S. Ohm and J.A. Hinton, *Non-thermal emission from pulsar-wind nebulae in starburst galaxies.*, **429** (2013) L70 [1210.8370].

[7] C.L. Carilli, *Free-free absorption towards the nucleus of NGC 253: further evidence for high pressures in the starburst nucleus.*, **305** (1996) 402.

[8] W. Pietsch, T.P. Roberts, M. Sako, M.J. Freyberg, A.M. Read, K.N. Borozdin et al., *XMM-Newton observations of <ASTROBJ>NGC 253</ASTROBJ>: Resolving the emission components in the disk and nuclear area*, **365** (2001) L174 [astro-ph/0010608].

[9] D.R. Wik, B.D. Lehmer, A.E. Hornschemeier, M. Yukita, A. Ptak, A. Zezas et al., *Spatially Resolving a Starburst Galaxy at Hard X-Ray Energies: NuSTAR, Chandra, and VLBA Observations of NGC 253*, **797** (2014) 79 [1411.1089].

[10] A. Abramowski, F. Acero, F. Aharonian, A.G. Akhperjanian, G. Anton, A. Balzer et al., *Spectral Analysis and Interpretation of the γ-Ray Emission from the Starburst Galaxy NGC 253*, **757** (2012) 158 [1205.5485].

[11] Z. Cao, D. della Volpe, S. Liu, Editors, :, X. Bi et al., *The Large High Altitude Air Shower Observatory (LHAASO) Science Book (2021 Edition)*, *arXiv e-prints* (2019) arXiv:1905.02773 [1905.02773].

[12] M.G. Aartsen, R. Abbasi, M. Ackermann, J. Adams, J.A. Aguilar, M. Ahlers et al., *IceCube-Gen2: the window to the extreme Universe*, *Journal of Physics G Nuclear Physics* **48** (2021) 060501 [2008.04323].

PoS(ICRC2023)815